ISSN 1028-334X, Doklady Earth Sciences, 2007, Vol. 413, No. 2, pp. 160–163. © Pleiades Publishing, Ltd., 2007.
Original Russian Text © G.E. Nekrasov, N.V. Rodionov, N.G. Berezhnaya, S.A. Sergeev, S.V. Ruzhentsev, O.R. Minina, B.G. Golionko, 2007, published in Doklady Akademii Nauk, 2007, Vol. 412, No. 5, pp. 661–664.

GEOLOGY

U–Pb Age of Zircons from Plagiogranite Veins in Migmatized Amphibolites of the Shaman Range (Ikat–Bagdarin Zone, Vitim Highland, Transbaikal Region)

G. E. Nekrasov[a], N. V. Rodionov[b], N. G. Berezhnaya[b], S. A. Sergeev[b], S. V. Ruzhentsev[a], O. R. Minina[c], and B. G. Golionko[a]

Presented by Academician A.L. Knipper, March 29, 2006

Received March 29, 2006

DOI: 10.1134/S1028334X0702002X

The Ikat–Bagdarin zone is considered as the northeastern element of the Hercynian system in the western Transbaikal region [1]. In the present-day structure, the zone consists of a system of outliers composed of metamorphosed rocks at the roof of the Angara–Vitim batholith. The largest of them is the Bagdarin synform representing a complicated fold–thrust structure with different rock complexes juxtaposed to form a packet of tectonic nappes (Fig. 1). Its lower part (relative autochthon) is composed of the Sivokon–Tocher Complex. According to available data, the base of this complex in the Shaman Range is represented by apobasaltic albite–epidote–actinolite schists of the Sivokon Formation attributed conditionally to the Upper Riphean. The formation includes gabbroid, diorite, and plagiogranite bodies in the axial part of the range. Serpentinite veins occur in some places. All these rocks are united into an ophiolitic association [2–4]. Recent Sm–Nd isotopic studies of amphiboles, which replace the dark mineral in gabbro of the Shaman Range, and of plagioclases from gabbro–pegmatites yielded an isochron age of 545 ± 19 Ma, $\varepsilon_{Nd} = 0.7$ (MSWD = 0.72) [5].

Our studies show that the greenschist complex of the range was developed after gabbroids and irregularly migmatized amphibolites with their migmatized varieties localized largely at the southeastern contact of the gabbro massif.

[a] *Geological Institute, Russian Academy of Sciences, Pyzhevskii per. 7, Moscow, 119017 Russia; e-mail: nekrasov@ginras.ru*

[b] *Karpinsky All-Russia Research Institute of Geology, Srednii pr. 74, St. Petersburg, 199106 Russia*

[c] *Buryat Geological Institute, Siberian Division, Russian Academy of Sciences, ul. Sakh'yanovoi 6A, Ulan-Ude, 670024 Russia*

For isotopic dating of intensely metamorphosed rocks, we sampled and analyzed zircons from amphibole plagiogranites enclosed in migmatized amphibolites from the upper reaches of the Aunik River, a tributary of the Bagdarin River (Fig. 1). In this area, amphibolites and their migmatized varieties constitute an approximately 500-m-thick SE-dipping sheet bounded in the northwest and southeast by outcrops of Upper Devonian–Lower Carboniferous terrigenous rocks of the Tocher Formation (Fig. 1). Amphibole plagiogranites, which have been sampled for zircons, form a system of subparallel veins (1–3 cm thick) in migmatized amphibolites. Plagiogranites are composed of short-platy plagioclase crystals, allotriomorphic quartz, and platy brownish green hornblende all showing signs of recrystallization in the greenschist facies. This is reflected in deformation and actinolitization of plagioclase and hornblende, as well as in quartz deformation and granulation. The substrate of migmatized amphibolites is characterized by a granoblastic texture and composed of brownish green magnesian hornblende and plagioclase. In slightly altered varieties, secondary transformations of the plagioclase are reflected in the replacement of the core by a mixture of epidote and leucoxene. Rims of plagioclase and hornblende are replaced by aggregates of small-platy actinolite. More intensely altered varieties are transformed in thin zones (0.5–1.0 cm thick) into a fine-banded foliated aggregate of albite, epidote, and actinolite. Quartz and carbonate occur as small lenses and spots.

The zircon monofraction is represented by light pink prismatic euhedral crystals of the hyacinth habit. The fraction is dominated by transparent crystals. Dull varieties constitute approximately 20%. The crystals are 100–200 μm long with an elongation coefficient of 1.5 to 3.0.

The cathode luminescence treatment of zircons reveals their two-phase state. They consist of a zoned

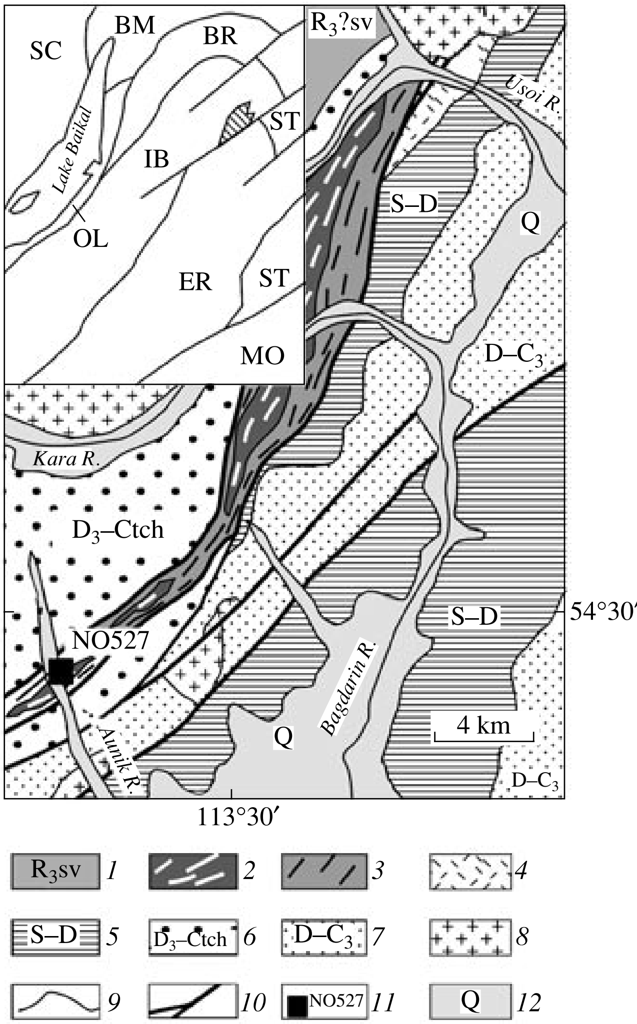

Fig. 1. Schematic structure of the Bagdarin area of the western Transbaikal region. (*1*) Terrigenous flyschoid Sivokon Formation; (*2, 3*) greenschist complex of the Shaman Range developed after gabbroids and migmatized amphibolites, respectively; (*4*) felsites and basalts of the Usoi Formation (probably Vendian–Cambrian); (*5*) carbonate rocks of the Orochen Formation; (*6*) terrigenous rocks of the Tocher Formation, including rudaceous varieties with greenschist, amphibolite, and granite pebbles; (*7*) terrigenous rocks of Yakshin and Bagdarin formations; (*8*) granites of the Vitimkan Complex; (*9*) boundaries of formations and intrusive complexes; (*10*) faults; (*11*) zircon sampling sites of plagiogranites and their numbers; (*12*) Quaternary sediments. Letters in the inset: (SC) Siberian Craton; terranes: (BM) Baikal–Muya, (BR) Barguzin, (OL) Ol'khon, (IB) Ikat–Bagdarin, (ER) Eravna, (ST) Stanovoi; (MO) Mongol–Okhotsk belt. Shaded area designates the Bagdarin synform.

core (60–180 μm across) enclosed in light-colored zoned envelopes of variable width (from 5 to 77 μm). The preservation degree of primary zoning in cores is variable. Many of them are partly recrystallized. Under the transmitted light, the core boundary is frequently marked by mineral particles and gas inclusions. In the cathode luminescence image, the core–envelope interface is black. Cores enclose melt and gas inclusions and apatite. The fissured envelopes contain gas and less common melt inclusions.

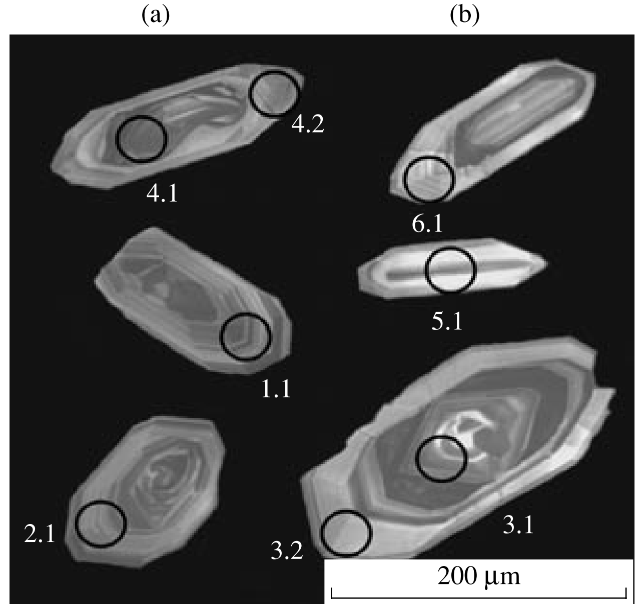

Fig. 2. Cathode luminescence images of examined zircons of the (a) first and (b) second groups from plagiogranite sample N0527 with analytical points.

In cores, the U and Th contents are 146–264 and 68–166 ppm, respectively (Th/U = 0.48–0.65). In the envelopes, the respective values are 80–179 and 17–85 ppm (Th/U = 0.22–0.49).

Depending on the absence (or presence) of cores, the structure of envelopes, and Th/U values, the examined zircons may conditionally be divided into two groups (Fig. 2). Zircons of the first group (Fig. 2a) are dominant. All of them have cores, thin rhythmical zoning in envelopes, and higher Th/U values (0.65 and 0.85 in cores and finely zoned envelopes, respectively). In contrast to zircons of the first group, some of their counterparts from the second group (Fig. 2b) are characterized by the absence of cores (point 5.1, Fig. 2b), development of wide continuous zones in the envelopes, and lower Th/U values (0.48 in the core and 0.34–0.22 in envelopes).

We analyzed the following objects: (1) the core (point 4.1) and finely zoned envelope (points 1.1, 2.1, 4.2) in zircons of the first group (Fig. 2a); (2) the core (point 3.1) and zoned envelope (points 3.2, 5.1, 6.1) in crystals of the second group (Fig. 2b).

Zircons were dated by the U–Pb method using the SHRIMP-II ionic microprobe at the Center of Isotopic Research of the Karpinsky All-Russia Research Institute of Geology. Hand-picked zircon grains were placed into epoxy resin together with grains of the zircon standards TEMORA and 91 500. Then, zircon grains were ground and polished approximately up to

U–Pb SHRIMP measurements of zircons from plagiogranites in migmatized amphibolites of the Shaman Range

Analytical point	$^{206}Pb_c$, %	U	Th	$^{232}Th/^{238}U$	$^{206}Pb^*$, ppm	Age, Ma (1σ)				Discordance, %	(1) $^{207}Pb^*/^{235}U$	±%	(1) $^{206}Pb^*/^{238}U$	±%	Correlation coefficient (rel. u.)
		ppm				$^{206}Pb/^{238}U$		$^{207}Pb/^{206}Pb$							
N05.27.1.1	0.41	226	114	0.52	32	979.9	±10	871	±83	–11	1.541	4.1	0.1642	1.1	0.263
N05.27.2.1	–0.55	127	31	0.26	17.5	963	±13	1014	±140	5	1.62	6.8	0.1611	1.5	0.218
N05.27.3.1	0.27	146	68	0.48	20.9	991	±12	888	±97	–10	1.573	4.9	0.1662	1.3	0.271
N05.27.3.2	0.00	80	17	0.22	11.3	977	±15	1008	±86	3	1.643	4.6	0.1636	1.7	0.372
N05.27.4.1	0.28	264	166	0.65	36	946.6	±9	947	±67	0	1.54	3.4	0.1582	0.99	0.287
N05.27.4.2	0.99	179	85	0.49	19.6	767	±10	660	±180	–14	1.072	8.7	0.1263	1.4	0.160
N05.27.5.1	–0.11	86	29	0.34	12.6	1015	±15	891	±81	–12	1.616	4.2	0.1705	1.6	0.368
N05.27.6.1	0.50	95	21	0.23	13.4	972	±15	820	±150	–16	1.49	7.6	0.1628	1.6	0.213

Note: (Pb_c, Pb*) proportions of common and radiogenic lead, respectively. Accuracy in standard calibration is 0.92%. (1) A correction for common lead was introduced using data on ^{204}Pb.

half of their thickness. Optical (transmitted and reflected light) and cathode luminescence images reflecting the internal structure and zoning patterns of zircon grains were used for selecting areas (points) at their surfaces for the analysis.

The U/Pb values were measured with the SHRIMP-II microprobe using the technique described in [6]. The intensity of the primary beam of molecular negatively charged oxygen ions was 6.5 nA. The diameter of the spot (crater) was 25 μm. The data obtained were processed using the SQUID program [7]. The U–Pb ratios were normalized to the value of 0.0668 assigned to the zircon standard TEMORA, which corresponds to its age of 416.75 Ma [8]. The accuracy of single measurements (ratios and ages) is quoted at the 1σ level, and errors of calculated concordant ages are given at a 95% confidence level. The concordia plots were constructed using the ISOPLOT/EX program [10].

The measurement results are presented in the table and shown in the diagram with U–Pb concordia (Fig. 3). Measurements at two points in the cores of crystals (3.1, 4.1) and at five points in the central parts of zoned rims (1.1, 2.1, 3.2, 5.1, 6.1) yielded the concordant age of 971.9 ± 14 Ma for crystals of both groups (Fig. 3). The concordant age of 760 ± 20 Ma was obtained only for point 4.2 in the peripheral part of the zoned rim in one of the crystals of the first group.

The obtained data suggest that the migmatized amphibolite complex of the Shaman Range belongs to the pre-Late Riphean basement of the Ikat–Bagdarin

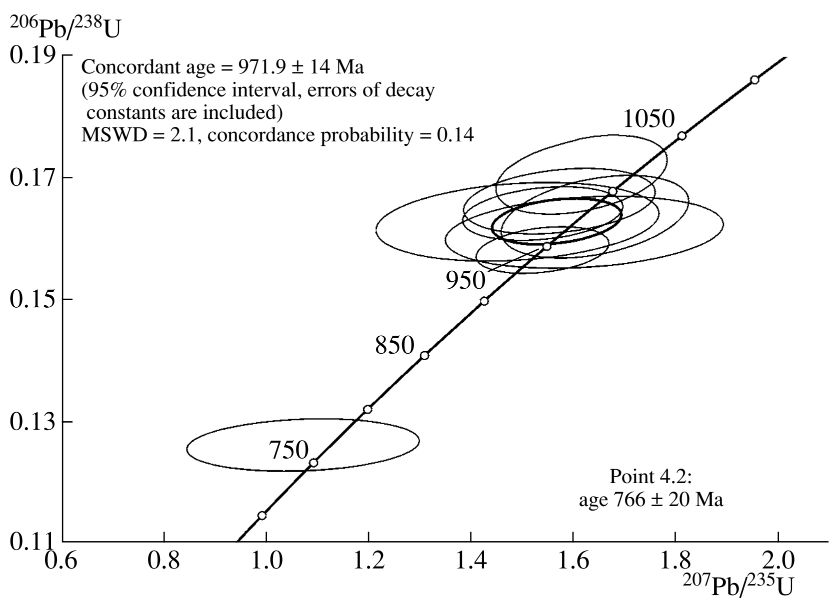

Fig. 3. Diagram with concordia for zircons from plagiogranite sample N0527.

zone. At the Early–Middle Paleozoic transition, this basement exhumed in response to the formation of the Bagdarin zone thrust and delivered detrital material of amphibolites, gabbro, and granites to the Tocher basin.

ACKNOWLEDGMENTS

This work was supported by the Russian Foundation for Basic Research, project nos. 05-05-65027 and 05-05-97228.

REFERENCES

1. S. V. Ruzhentsev, O. R. Minina, V. A. Aristov, et al., in *Problems of the Tectonics of Central Asia* (Geos, Moscow, 2005), pp. 171–196 [in Russian].
2. G. L. Mitrofanov and N. N. Mitrofanova, in *Magmatism and Metamorphism in the BAM Zone and Their Role in the Formation of Mineral Resources* (Nauka, Novosibirsk, 1983), pp. 60–63 [in Russian].
3. L. M. Parfenov, A. N. Bulatov, and I. V. Gordienko, Tikhookean. Geol. **15** (4), 3 (1996).
4. M. I. Grudinin, *Mafic–Ultramafic Magmatism in the Baikal Mountainous Region* (Nauka, Novosibirsk, 1997) [in Russian].
5. E. Yu. Rytsk, A. F. Makeev, E. S. Bogomolov, et al., in *Isotopic Geochronology for the Solution of Problems of Geodynamics and Ore Formation* (St. Petersburg, 2003), pp. 440–442 [in Russian].
6. I. S. Williams, Rev. Econ. Geol **7**, 1 (1998).
7. K. R. Ludwig, *SQUID 1.00, A User's Manual* (Berkeley Geochronology Center Spec. Pub., Berkeley, 2000).
8. L. P. Black, S. L. Kamo, J. N. Aleinikov, et al., Chem. Geol. **200**, 155 (2003).
9. G. W. Wetherill, Trans. Am. Geophys. Union **37**, 320 (1956).
10. K. R. Ludwig, *User's Manual for Isoplot/Ex. Vers. 2.20. A Geochronological Toolkit for Microsoft Excel* (Berkeley Geochronology Center Spec. Publ., Berkeley, 1999).